Original

Oxidative Stress-induced Interaction between Autophagy and Cellular Senescence in Human Keratinocytes

Masahiro Yamaguchi[1, 2)], Hiroshi Kajiya[2, 3)], Rui Egashira[1,2)], Madoka Yasunaga[2, 4)], Kanako Hagio-Izaki[2, 5)], Ayako Sato[2, 6)], Takuya Toshimitsu[2,7)], Toru Naito[1)] and Jun Ohno[2)]

[1)]Section of Geriatric Dentistry, Department of General Dentistry, Fukuoka Dental College, Fukuoka, Japan

[2)]Research Center for Regenerative Medicine, Fukuoka Dental College, Fukuoka, Japan

[3)]Section of Cellular Physiology, Department of Physiological Science and Molecular Biology, Fukuoka Dental College, Fukuoka, Japan

[4)]Section of Orthodontics, Department of Oral Growth and Development, Fukuoka Dental College, Fukuoka, Japan

[5)]Section of General Dentistry, Department of General Dentistry, Fukuoka Dental College, Fukuoka, Japan

[6)]Section of Oral Implantology, Department of Oral Rehabilitation, Fukuoka Dental College, Fukuoka, Japan

[7)]Dentistry for the Disabled, Department of Oral Growth and Development, Fukuoka Dental College, Fukuoka, Japan

Correspondence to:Dr Jun Ohno

Research Center for Regenerative Medicine, Fukuoka Dental College, 2-15-1 Tamura, Sawara-ku, Fukuoka, Fukuoka 814-0193, Japan;

Tel: +81 928010411 (Ext 684);

Fax: +81 928014909 ;

E-mail: johno@college.fdcnet.ac.jp

Running title: Oxdative stresss-induced cellular senescence

Abstract : Oxidative stress in keratinocytes induces cytoprotective events, such as autophagy and cellular senescence. The present study investigated whether an induction of autophagy and cellular senescence can be observed in oxidative-stressed keratinocytes to allow those cells to maintain a cytoprotecitve state. We examined that the effect of various inhibitors on the induction of both autophagy and senescence in H_2O_2-treated HaCaT cells via Western blotting and immunocytochemical assays. H_2O_2-treated cells exhibited increased expression of the senescent markers, p21 and Decades (Dec1), in addition to increased and decreased numbers of senescence-associated β-galactosidase (SA-β-gal) – and Ki-67–positive cells, respectively. These senescent cells also displayed upregulation of the autophagy marker, LC3-II. Attenuation of LC3-II expression using 3-methyladenin inhibited H_2O_2-autophagy and cellular senescence. Our Western blotting results revealed that H_2O_2-induced autophagy was regulated independently by the negative feedback pathway of a mammalian target of rapamycin. By contrast, H_2O_2-induced autophagy and cellular senescence depended on the activation of the p38 mitogen-activated protein kinase α (MAPKα) pathway mediated by the intracellular reactive oxygen species (ROS) production. Furthermore, a suppression of autophagy by 3-methyladenine promoted an induction of apoptosis in H_2O_2-treated cells, suggesting that autophagy, in association with the cellular senescence, may induce the cytoprotection under the oxidative stress. Our findings suggest that the acceleration of both events may allow

stressed cells to maintain the cytoprotective effects and may be regulated, in part, by p38 MAPK activation through the intracellular production of ROS.

Key words: cellular senescence, autophagy, oxidative stress, reactive oxygen species (ROS)

Introduction

Cells respond to stress via several processes ranging from cytoprotective functions that activate signaling pathways to cytotoxic events that elicit apoptosis to eliminate damaged cells. It is becoming apparent that macroautophagy (hereafter referred to as autophagy), which involves the formation of double-membrane vesicles (autophagosomes) and facilitates the maintenance of cellular homeostasis through cytoplasmic and organelle turnover, is a major component of the cellular stress response [1, 2]. Cells exposed to oxidative stress exhibit increased autophagy activity [3, 4]. However, the mechanisms by which oxidative stress induces increased autophagy have remained unclear.

Cellular senescence is a process by which cells remain in a state of cell growth arrest, but maintain metabolicalic activity with several distinctive morphological changes, such an enlarged and flattened cell shape and the ability to be visualized using the widely accepted and used marker, senescence-associated beta-galactosidase (SA-β-gal) [5-8]. In addition to autophagic induction, oxidative stress also induces cellular senescence [9]. It has been suggestively reported that the molecular pathways regulating

autophagy and cellular senescence in the cells exposed to oxidative stress may be interconnected [10-15].

Oral epithelium of the oral mucosa primarily consists of multilayered renewing keratinocytes, and this structure forms the extremely important barrier which is responsible for the defensive responses against various environmental stimulators, such as heat, cold, trauma, radiation, and infection. Recent studies indicate that autophagy plays a crucial role on keratinocyte biology and pathology [16-18]. Oxidative stress generates intracellular accumulation of H_2O_2 that could enhance autophagy to eliminate the oxidative-damaged mitochondria and nuclei, and initiate the cellular senescence in keratinocytes [19]. However, an inducible interaction between autophagy and keratinocyte senescence remains unclear, under oxidative stress conditions.

The levels of reactive oxygen species (ROS) increase in response to different types of stresses, including oxidative stress [20, 21]. During exposure to oxidative stress, increased ROS may lead to the acceleration of both autophagy and cellular senescence [22, 23]. However, the precise mechanisms of the ROS-mediated induction of autophagy and cellular senescence during exposure to the oxidative stress remain unclear. This study aimed to elucidate whether an induction of both autophagy and cellular senescence, through increased production of intracellular ROS, can be observed in oxidative-stressed keratinocytes and whether both inducible events can allow stressed cells to maintain a cytoprotecitve state.

Materials and Methods

Reagents and antibodies

SB203580 (4-[4-fluorophenyl]-2-[4- methylsulfinylphenyl]-5- [4-pyridyl] 1H-imidazole SB) was purchased from LC Laboratories (Woburn, MA, USA). 3-Methyladenine (3-MA), N-acetylcysteine (NAC), pifithrin-α (PFTα), Hoechst 33324, and the monoclonal antibody against β-actin (ACTB) were purchased from Sigma (St. Louis, MO, USA). Antibodies against Decades (Dec1) and $p21^{Cip1/WAF1}$ (p21) were obtained from Santa Cruz Biotechnology, Inc. (Santa Cruz, CA, USA). Antibodies against p38 mitogen-activation protein kinase α (p38 MAPKα), phosphorylated p38 MAPKα (p-p38 MAPKα), phosphorylated p70S6K (p-p70S6K), phosphorylated 4E-BP1 (p-4E-BP1), phosphorylated AKT (s473) (p-AKT), Ki-67, p53, phosphorylated p53 (p-p53), cleaved poly (ADP-ribose) polymerase (PARP), B-cell lymphoma 2 (Bcl-2), and Bcl-2-associated X protein (Bax) were purchased from Cell Signaling Technology (Delaware, CA, USA). Rabbit polyclonal antibodies against microtubule-associated protein light chain 3 (LC3) and beclin-1 (BECN1) were purchased from MBL (Tokyo, Japan). Annexin V, Alexa Fluor 568 conjugate, Alexa Fluor 488-conjugated goat anti-rabbit IgG and rabbit anti-mouse IgG were purchased from ThermoFisher Scientific (Commonwealth, MA, USA).

Cell culture

HaCaT cells, a human keratinocyte line, were maintained in high-glucose Dulbecco's modified Eagle's medium (DMEM; Wako, Osaka, Japan) supplemented with 10% (v/v) fetal bovine serum (FBS; HyClone Laboratories, Inc., South Logan, UT, USA) and 1% penicillin and streptomycin (Anti-Anti; Invitrogen, Carlsbad, CA, USA) at 37°C in a humidified incubator with 5% CO_2. For H_2O_2 stimulation, HaCaT cells at approximately 80% confluence were exposed to 300 μM H_2O_2 diluted in DMEM supplemented with 10% FBS for 0 - 72 h.

Cell viability assay

To determine cell viability, HaCaT cells treated with or without H_2O_2 were washed with phosphate-buffered saline (PBS), harvested from the dishes via trypsinization, resuspended in PBS, and diluted 1:1 in 0.4% trypan blue solution. Cell viability was calculated using a Countess® Automated Cell Counter (Invitrogen) according to the manufacturer's procedures.

Senescence-associated β-galactosidase (SA-β-gal) staining

SA-β-gal staining in HaCaT cells was performed using a Senescence Cells Histochemical Staining Kit (Sigma-Aldrich), according to the manufacturer's instructions. Positive senescent cells were identified as colored cells using light

microscopy. A hundred cells were counted in 5 random fields to determine the percentage of SA-β-gal positive cells.

Immunocytochemistry

Antibodies against Ki-67, LC3, and cleaved PARP were used in immunocytochemistry. Cultured cells on 10-well glass slides were fixed with 4% paraformaldehyde for 10 min and washed in 0.1% Triton X-100 in PBS for 15 min. The cells were incubated with primary antibodies for 2 h at room temperature. After washing with PBS, the cells were incubated with anti-mouse IgG or anti-rabbit IgG with Alexa Fluor 488 at room temperature for 45 min. Furthermore, we performed a double immunofluorescent staining on the fixed cells comprising mixtures of cleaved PARP and annexin V. After an incubation of anti-cleaved PARP antibody, the cells were incubated a mixture of anti-rabbit IgG antibody conjugated to Alexa Fluor 488 and annexin V conjugated to Alexa Fluor 568. To visualize the nuclei, cells were counterstained with Hoechst 33324.

Western blot analysis

The cells were lysed in Cell Lysis Buffer (Cell Signaling Technology) containing a 1× protease/phosphatase inhibitor cocktail (Cell Signaling Technology). The protein content was measured using a protein assay kit (Pierce, Hercules, CA, USA). Protein

samples (15 μg), together with a protein marker (Precision Plus Protein Western C Standards; Bio-Rad, Richmond, CA, USA), were separated on 12% Mini-protean TGX gels (Bio-Rad) for 30 min at 200V.The separated proteins were transferred to a polyvinylidene fluoride membrane for 3 min using the Trans-Blot Turbo Transfer system (Bio-Rad) with Trans-Blot Transfer Packs. Western blots were processed on the iBind Western System (Life Technologies, Carlsbad, CA, USA). The incubated membranes were developed using an enhanced chemiluminescence system (Signal Fire Plus ECL Reagent; Cell Signaling Technology). The band density was quantified using the NIH-Image J software and normalized to that of ACTB.

Analysis of intracellular ROS production

A fluorescent assay of intracellular ROS production was determined using a CellROX® Green Reagent (Invitrogen) according to the manufacturer's manual. The production of intracellular ROS was detected as green-stained cells via fluorescence microscopy.

Statistical analysis

A statistical analysis used STAT VIEW (STAT VIEW for Windows, version 5). The analysis was performed with one-way analysis of variance (ANOVA) and Scheffe's multiple comparison test or Student's t-test to determine the statistical differences

among the samples. Data are presented as the mean ± standard deviation (SD) and *P* values < 0.05 were considered to be statistically significant.

Results

Induction of cellular senescence in HaCaT cells exposed to H_2O_2

Exposure of cells to H_2O_2 can result in stress induced premature senescence (SIPS) [24]. To investigate whether oxidative stress can induce in cellular senescence in HaCaT cells, we treated cultured HaCaT cells with 300 μM H_2O_2 for 0–72 h. We first examined the effect of H_2O_2 on the viability of HaCaT cells via trypan blue dye exclusion (Fig. 1A), wherein we observed a significant decrease in the cell viability during the treatment with H_2O_2. After 12 and 24 h of exposure to H_2O_2, cell viability was decreased by approximately 20% and 40%, respectively. Fig. 1B shows the representative phase contrast images of HaCaT cells treated with or without H_2O_2. H_2O_2–treated cells exhibited an enlarged cell size and the accumulation of cytoplasmic granules, reflecting some of the morphological characteristics of cellular senescence [25-27].

SA–β–gal is the most widely known biomaker of cellular senescence [28]. We examined SA–β–gal staining in HaCaT cells treated with or without 300 μM H_2O_2 for 24 h (Fig. 2A). Microscopic analysis revealed an increase in the number of SA–β –gal–positive H_2O_2–treated cells (0.0 ± 0.0% [control] versus 11.2 ± 4.4% [treated]; n=3, p =

0.025) (Fig. 2B). We also examined changes in the number of Ki-67–positive cells among H_2O_2–treated cells, as a recent study has proposed that Ki-67 as a candidate marker for cellular senescence [29]. Immunofluorescence analysis revealed a decrease in the number of Ki-67-positive cells among those treated with 300 μM H_2O_2 for 24 h (39.9 ± 5.5% [control] versus 11.2 ± 3.2% [treated]; n = 3, p = 0.041) (Figs. 3Aand B). These results suggest that H_2O_2-treated cells may have a decreased proliferative activity.

We next performed Western blotting assay of senescence-related proteins in HaCaT cells treated with or without 300 μM H_2O_2. The protein expression levels of p21 and Dec1, the established markers for senescence [13, 30], were enhanced after 24 h of H_2O_2 treatment (Fig. 4). These results are in accordance with those of phase contrast imaging, SA-β-gal staining, and Ki-67 immunostaining.

H_2O_2 treatment induces autophagy in HaCaT cells

Cellular stress induces autophagy in cells as one of cellular survival program [1, 2]. We examined whether 300 μM H_2O_2 could induce autophagy in HaCaT cells. LC3 exists in two molecular forms, LC3-I (18 kDa) is cytosolic, whereas LC3-II (16 kDa) binds to the autophagosomal membrane and serves as a marker of defective autophagosome formation [31].

Following treatment with 300 μM H_2O_2 for 0 - 72 h, respectively, LC3-II expression increased in a time-dependent manner, peaking at 24 h, and then declining

(Fig. 5). A time point of 24 h for increased LC3-II expression is in line with that for senescence induction.

Autophagosome formation was examined further by fluorescence microscopic analysis of immunocytostaining with anti-LC3 antibody. The amount of LC3-II directly correlated with the number of autophagosomes [26]. H_2O_2-treated cells exhibited characteristic punctate LC3-II fluorescence, whereas the green fluorescence of untreated (control) cells remained cytosolic and diffuse (Fig. 6A). As shown in Fig. 6B, the number of autophagosomes increased in HaCaT cells treated with 300 μM H_2O_2 compared with that in untreated (control) cells (4.5 ± 1.8 % [control] versus 59.2 ± 9.6% [treated]; n = 3, p = 0.016). These results indicate that HaCaT cells treated with H_2O_2 can induce both senescence and autophagy in HaCaT cells.

The induction of cellular senescence regulated by H_2O_2-induced autophagy

To elucidate whether autophagy could regulate oxidative stress-induced senescence through the expression of senescent markers, the expression of LC3-II in HaCaT cells was pharmacologically downregulated using 3-MA, an inhibitor of PI3K class III [32], prior to their exposure to H_2O_2. HaCaT cells were preincubated with 5 mM 3-MA for 2 h and then treated with 300 μM H_2O_2 for 24 h. 3-MA pretreatment reduced the expression of LC3-II (Fig. 7). In line with the Western blotting data, 3-MA diminished the formation of LC3 puncta (Fig. 8). As shown in Fig. 9A, the percentage of

LC3-positive autophagosomes was remarkably diminished in 3-MA pretreated HaCaT cells (50.7 ± 6.5% [H_2O_2-treated] versus 13.7 ± 6.1% [3-MA pretreated]; n=3, p=0.0082). These results indicate that 3-MA pretreatment can pharmacologically reduce the induction of autophagy in H_2O_2-treated HaCaT cells.

We next investigated whether the pharmacological suppression of autophagy could affect H_2O_2-induced cellular senescence in HaCaT cells. Fig. 7 shows that 3-MA pretreatment attenuated the expression of both p21 and Dec1. In line with the Western blotting data, the intensity of both SA-β-gal and Ki-67 staining indicated anti-senescent activity. 3-MA–pretreated cells exhibited less SA-β-gal staining than cells that were not pretreated after exposure to H_2O_2 (4.5 ± 1.5 % [3-MA– pretreated] versus 11.8 ± 3.9 % [no 3-MA–pretreamtnet]: n=3, p=0.035) (Fig. 9B left). By contrast, the number of Ki-67-positive cells was elevated among HaCaT cells pretreated with 3-MA compared with the findings for cells that were not pretreated (42.4 ± 6.9 % [3-MA–pretreated] versus 11.0 ± 3.2% [no 3-MA–pretreatment]: n=3, p=0.024) (Fig. 9B right). These findings suggest that autophagy may regulate oxidative stress-induced senescence through p21 and Dec1 expression.

H_2O_2-induced autophagy in HaCaT cells is regulated independently by the mammalian target of rapamycin (mTOR) pathway

Recent studies indicated that autophagy was activated during starvation and oncogenic stress-induced senescence in association with negative feedback in the mTOR pathway [33]. We therefore investigated whether H_2O_2 treatment could accelerate autophagy suppressed by the mTOR pathway through analysis of the levels of p-p70S6K, p-4E-BP1, and p-AKT (s473), as p70S6K and 4EBP1 are the downstream targets of mTOR complex 1 (mTORC1) and p-AKT (s473) is a phosphorylated product of mTOR complex 2 (mTORC2) [33]. HaCaT cells treated with H_2O_2 increased the autophagy activity, as the H_2O_2-treated cells displayed increased expression of both LC3-II and BECN1 (also known as Atg6) (Fig. 10). BECN1 is involved in the formation of the autophagosomes [13, 33]. Conversely, the levels of p-p70S6K, p-4E-BP1, and p-AKT expression were not changed by the treatment of HaCaT cells with H_2O_2 treatment (Fig. 10). These findings indicate that unlike starvation and oncogenic stresses, H_2O_2 may promote autophagy independently of the negative feedback regulation of the mTOR pathway.

Production of intracellular ROS can mediate H_2O_2-induced autophagy and cellular senescence

Growing body of the evidence has revealed that the intracellular ROS production is implicated in mediating the induction of both autophagy and cellular senescence in response to various cellular stresses [13, 34, 35]. We examined the effect of intracellular

ROS production on the induction of both autophagy and cellular senescence. First, we investigated whether the HaCaT cells treated with 300 μM H_2O_2 for 24 h induces a persistent increase in the intracellular production of ROS by the fluorescent assay of CellROX reagents. As shown in Fig. 11, H_2O_2-treated cells displayed increased levels of intracellular ROS, whereas its production was attenuated in the cells treated with or without H_2O_2 and NAC. These findings indicate that NAC may function as an effective antioxidant to inhibit the H_2O_2-induced intracellular ROS production.

Western blotting analysis revealed decreased expression of LC3-II and BECN1 in NAC treated cells (Fig. 12). A decline in the production of intracellular ROS was also affected in senescence-related proteins. As shown in Fig. 13, the expression of p21 and Dec1 was decreased in the cells treated with H_2O_2 and NAC compared with that in cells treated with H_2O_2 alone. These findings suggest that ROS-induced cellular senescence may be suppressed in parallel with the reduction of ROS-induced autophagy.

Upregulation of p38 MAPK via ROS production increases H_2O_2-induced autophagy and p21 expression

Recent studies suggest that H_2O_2-induced p21expression may be regulated by the p53/p21 pathway or by the activation of p38 MAPKα [36-40]. We first examined whether H_2O_2-induced intracellular ROS production is related to both p53 and p38 MAPKα in HaCaT cells. As shown in Fig. 14, increased expression of both p-p53 and p-p38

MAPKα was observed in H_2O_2-treated cells. Their activation was inhibited by the specific ROS inhibitor NAC, indicating that p53 and p38 MAPKα expression in H_2O_2-treated cells are activated by intracellular ROS production.

We next examined the involvement of the p53/p21 pathway in the upregulation of p21 expression in H_2O_2-treated cells using the p53-specific inhibitor PFTα [41]. PFTα treatment inhibited p-p53 expression in H_2O_2-treated cells, whereas p21 expression remained elevated (Fig. 15). These findings suggest that H_2O_2-induced p21 expression may be upregulated independently by the p53 pathway. To elucidate the effect of p38 MAPK activation on p21 expression in H_2O_2-treated cells, we assessed the changes in p21 expression in the cells treated with or without SB 203580, a specific inhibitor of p38 MAPK [13, 33]. In addition to decreased p-p38 MAPKα expression, SB203580 treatment attenuated the expression of both p21 and LC3-II in H_2O_2-treated cells (Fig. 16), suggesting that p38 MAPK activation may regulate, at least in part, both p21and LC3-II expression during the oxidative stress. Inhibition of p38 MAPK activity reduced the percentage of SA-β-gal-positive cells H_2O_2-treated cells with (5.4 ± 1.6 % [H_2O_2 and SB203580 treatment] versus 12.2 ± 3.6 % [H_2O_2 alone]: n=3, p=0.038) (Fig. 17 left). Furthermore, SB 203580 treatment increased the percentage of Ki-67-positive cells than the cells without the inhibitor (37.6 ± 6.5 % [H_2O_2 and SB203580 treatment] versus 20.3 ± 6.3 % [H_2O_2 alone]: n=3, p=0.041) (Fig. 17 right). These findings suggest

that both autophagy and cellular senescence induced by the oxidative stress may be mediated, in part, by p38 MAPK activation via intracellular ROS production.

Autophagy suppression attenuates capacity of H_2O_2-treated cells to protect to the cellular stress

An induction of both autophagy and cellular senescence can lead to the cytoprotective effects under various stress conditions. To elucidate whether both autophagy and senescence are contributed to the cellular adaptation in H_2O_2-treated cells, we examined an apoptotic cell death in autophagy-depleted cells. We first performed a dual cytochemical method to cytochemically detect apoptotic cells using a mixture of flurorescence-labelled annexin V and cleaved PARP antibody. Both annexin V and cleaved PARP are well-known as a cytochemical marker for apoptosis. In H_2O_2-treated cells with 3-MA pretreatment, annexin V and cleaved PARP were observed as cytoplasmic and intranuclear fluorescence, respectively, while the cells untreated or treated with H_2O_2 alone showed no fluorescence (Fig. 18). In Western blotting assays (Fig. 19), the expression of cleaved PARP and Bax, known as apoptotic markers, were accelerated by 3-MA pretreatment. In contrast, the expression of Bcl-2, anti-apoptotic marker, was decreased in 3-MA-pretreated cells. These results indicate that a reduction of autophagy by 3-MA-pretreatmnet promotes an induction of apoptotic

cell death in H_2O_2-treated cells, suggesting that autophagy, in association with the cellular senescence, induce the cytoprotection under the oxidative stress.

Discussion

In this study, we demonstrated that oxidative stress induced both cellular senescence and autophagy in human keratinocytes via intracellular ROS-mediated p38 MAPK activation. We presented three lines of evidence to support this concept. First, H_2O_2-treated HaCaT cells exhibited an acceleration of both cellular senescence and autophagy. Second, pharmacological innibition of autophagy attenuated the induction of cellular senescence. Third, downregulation of intracellular ROS production and p38 MAPK activation revealed decreased the expression of both autophagy- and senescence-related factors.

A number of papers have provided indirect or circumstantial evidence for the collateral induction of autophagy and senescence. However, these studies reported controversial results regarding the effect of autophagy on the induction of cellular senescence [10, 11, 14, 15, 38]. Some groups have suggested that accelerated autophagy may induce the cellular senescence in stressed cells [14, 15], whereas others have proposed an association of autophagy impairment with the induction of senescence in stressed cells [9, 10]. Our findings of a close relationship between autophagy and cellular senescence provide additional support for the former hypothesis.

It is well known that cellular senescence is primarily manipulated through the canonical p53/p21 signaling pathway [22, 42]. We confirmed that increased production of intracellular ROS facilitated p-p53 expression in H_2O_2-treated cells. Treatment with PFTα, a specific inhibitor of p53, reduced p-p53 expression in the H_2O_2-treated cells, whereas no effect was observed on p21 expression. These findings suggest that increased expression of p21 due to oxidative stress may be regulated via the p53-independent signaling, although a recent study demonstrated that increased transcriptional activity of p53 leads to upregulation of p21 [43]. In our Western blotting assay, we also found increased expression of p-p38 MAPK in oxidative stressed cells, indicating that intracellular ROS production in response to H_2O_2 treatment can induce p38 MAPK activity. Moreover, p21 and LC3-II expression in the H_2O_2-treated cells was decreased by treatment with an inhibitor of p38 MAPK, indicating that the expression of autophagy and senescence markers induced by the oxidative stress is regulated in part by the p38 MAPK activation. These findings suggest that the association between autophagy and cellular senescence, induced by the oxidative stress, may be mediated by p38 MAPK activity through the increased production of intercellular ROS.

It was generally acknowledged that, under the cellular stress, the cells undergo a series of genetic and metabolic changes that allow them to the induction of the cytoprotective functions [44, 45]. Consistent with these studies, we showed that HaCaT cells suppressed autophagy by pretreatment with 3-MA revealed upregulation of

apoptotic markers, such as cleaved PARP, annexin V, and Bax, by cytochemical and Western blotting assays, indicating that inhibition of autophagy augments cytotoxicity by triggering apoptosis. Despite present controversies on the exact role of autophagy and cellular senescence in the process of the cellular stress [45, 46], either by cell protection or contrarily by inducing cell death, a majority of studies have been indicated that autophagy is a protective mechanism associated with increased anti-apoptotic effects [15, 23, 27, 46]. Our data suggest that the oxidative-induced autophagy, in association with the induction of cellular senescence, may contribute to facilitate the cytoprotective effects on stressed cells. Recent studies have indicated the correlation between p21 and cell cycle control [47 – 49]. It has been known that p21 actively arrests cell cycle progression in G0 or G1 phase. Therefore, our results indicating the cytoprotective effect may be the result of cell cycle arrest by an upregulation of autophagy-induced p21 expression under the oxidative stress, while the addition of 3-MA may restore cell cycle progression.

A possible limitation of this study could be the lack of evidence regarding a direct pathway or factors controlling the interrelationship between autophagy and cellular senescence in oxidative stressed cells. However, we examined the indirectly decreased expression of senescent factors, p21 and Dec1, via pharmacological inhibition of autophagy. Moreover, we speculated that upregulation of both atuphagy and senescence activity was mediated by p38 MAPK activation. However, the mechanism by which the

38 MAPK pathway can regulate both events remains unclear. Further studies are warranted to examine the mechanisms of cross-talk between autophagy and cellular senescence in the oxidative stressed keratinocytes.

In conclusion, the findings of this study will shed additional light on the interaction between autophagy and cellular senescence in oxidative stressed cells. The acceleration of both events may allow stressed cells to be cytoprotective and may be regulated, in part, by p38 MAPK activation through the intracellular production of ROS.

Abbreviations

Dec1, Decades; SA-β-gal, senescence-associated β-galactosidase; MAPKα, p38 mitogen-activated protein kinase α; ROS, reactive oxygen species; 3-MA, 3-methyladenine; NAC, N-acetylcysteine; PFTα , pifithrin-α; β-ACTB, β-actin; PARP, poly (ADP-ribose) polymerase; Bcl-2, B-cell lymphoma 2; Bax, Bcl-2-associated X protein; LC3, microtubule-associated protein light chain 3; BECN1, beclin-1; PBS, phosphate-buffered saline; mTOR, mammalian target of rapamycin

Acknowledgments

We would like to thank Enago (www.enago.jp) for the English language review.

Conflicts of Interests

The authors declare that they have no competing interests.

References

1. Mizushima N, Levine B, Cuervo AM and J.klionsky D. Autophagy fights disease through cellular self-digestion. Nature 451: 1069-75, 2008
2. Cuervo AM, Bergamini E, Brunk UT, Droge W, Ffrench M and Terman A. Autophagy and aging: the importance of maintaining "clean" cells. Autophagy 1: 131-40, 2005
3. Dewaele M, Maes H and Agostinis P. ROS-mediated mechanisms of autophagy stimulation and their relevance in cancer therapy. Autophagy 6: 838-54. 2010
4. Azad MB, Chen Y and Gibson SB. Regulation of autophagy by reactive oxygen species (ROS): implications for cancer progression and treatment. Antioxid Redox Signal 11: 777-90. 2009
5. Debacq-Chainiaux F, Erusalimsky JD, Campisi J and Toussaint O. Protocols to detect senescence-associated beta-galactosidase (SA-betagal) activity, a biomarker of senescent cells in culture and in vivo. Nat Protoc 4: 1798-806. 2009
6. Dimri GP, Lee X, Basile G, M Acosta, G Scott, C Roskelley, E E Medrano, M Linskens, I Rubelj and O Pereira-Smith. A biomarker that identifies senescent human cells in culture and in aging skin in vivo. Proc Natl Acad Sci U S A 92: 9363-7. 1995
7. Collado M and Serrano M. Senescence in tumours: evidence from mice and humans. Nat Rev Cancer 10: 51-7. 2010
8. Collado M, Blasco MA and Serrano M. Cellular senescence in cancer and aging.

Cell 130: 223-33. 2007

9. Lu T and Finkel T. Free radicals and senescence. Exp Cell Res 314: 1918-22. 2008
10. Tsuchihashi NA, Hayashi K, Dan K, Goto F, Nomura Y, Fujioka M, Kanzaki S, Komune S and Ogawa K. Autophagy through 4EBP1 and AMPK regulates oxidative stress-induced premature senescence in auditory cells. Oncotarget 6: 3644-55. 2015
11. Kang HT, Lee KB, Kim SY, Choi HR and Park SC. Autophagy impairment induces premature senescence in primary human fibroblasts. PLoS One 6: e23367. 2011
12. Guo L, Xie B and Mao Z. Autophagy in Premature Senescent Cells Is Activated via AMPK Pathway. Int J Mol Sci 13: 3563-82. 2012
13. Gewirtz DA. Autophagy and senescence: a partnership in search of definition. Autophagy 9: 808-12. 2013
14. Luo Y, Zou P, Zou J, Wang J, Zhou D and Liu L. Autophagy regulates ROS-induced cellular senescence via p21 in a p38 MAPKalpha dependent manner. Exp Gerontol 46: 860-7. 2011
15. White E and Lowe SW. Eating to exit: autophagy-enabled senescence revealed. Gene Dev 23: 784-7. 2009
16. Buckingham EM, Carpenter JE, Jackson W, Zerboni L, Arvin AM and Grose C. Autophagic flux without a block differentiates varicella-zoster virus infection from

herpes simplex virus infection. Proc Natl Acad Sci USA 112: 256-61. 2015

17. Choi SR, Chung BY, Kim SW, Kim CD, Yun WJ, Lee MW, Choi JH and Chang SE. Activation of autophagic pathways is related to growth inhibition and senescence in cutaneous squamous cell carcinoma. Exp Dermatol 23: 718-24. 2014
18. Feldmeyer L, Hofbauer GF, Boni T, French LE and Hafner J. Mammalian target of rapamycin (mTOR) inhibitors slow skin carcinogensis, but impair wound healing. Br J Dermatol 166: 422-4. 2012
19. Deruy E, Gosselin K, Vercamer C, Martien S, Bouali F, Slomianny C, Bertout J, Bernard D, Pourtier A and Abbadie C. MnSOD upregulation induces autophagyic programed cell death in senescent keratinocytes. PLoS One 5: e12712. 2010
20. Debacq-Chainiaux F, Boilan E, Dedessus Le, Weemaels G and Toussaint O. p38(MAPK) in the senescence of human and murine fibroblasts. Adv Exp Med Biol 694: 126-37. 2010
21. Passos JF, Simillion C, Hallinan J, Wipat A and von Zglinicki T. Cellular senescence: unravelling complexity. Age 31: 353-63. 2009
22. Munoz-Espin D and Serrano M. Cellular senescence: from physiology to pathology. Nat Rev Mol Cell Biol 15: 482-96. 2014
23. Filomeni G, De Zio D and Cecconi F. Oxidative stress and autophagy: the clash between damage and metabolic needs. Cell Death Differ 22: 377-88. 2015
24. Cao C, Lu S, Kivlin R, Wallin B, Card E, Bagdasarian A, Tamakloe T, Wang WJ,

Song X, Chu WM, Kouttab N, Xu A and Wan Y. SIRT1 confers protection against UVB- and H2O2-induced cell death via modulation of p53 and JNK in cultured skin keratinocytes. J Cell Mol Med 13: 3632-43. 2009

25. Tchkonia T, Zhu Y, van Deursen J, Campisi J and Kirkland JL. Cellular senescence and the senescent secretory phenotype: therapeutic opportunities. J Clin Invest 123: 966-72. 2013
26. De Cecco M, Jeyapalan J, Zhao X, Tamamori-Adachi M and Sedivy JM. Nuclear protein accumulation in cellular senescence and organismal aging revealed with a novel single-cell resolution fluorescence microscopy assay. Aging 3: 955-67. 2011
27. Rodier F and Campisi J. Four faces of cellular senescence. J Cell Biol 192: 547-56. 2011
28. Young JJ, Patel A and Rai P. Suppression of thioredoxin-1 induces premature senescence in normal human fibroblasts. Biochem Biophys Res Commun 392: 363-8. 2010
29. Lawless C, Wang C, Jurk D, Merz A, Zglinicki Tv and Passos JF. Quantitative assessment of markers for cell senescence. Exp Gerontol 45: 772-8. 2010
30. Qian Y, Zhang J, Yan B and Chen X. DEC1, a basic helix-loop-helix transcription factor and a novel target gene of the p53 family, mediates p53-dependent premature senescence. J Biol Chem 283: 2896-905. 2008
31. Nakagawa I, Amano A, Mizushima N, Yamamoto A, Yamaguchi H, Kamimoto T,

Nara A, Funao J, Nakata M, Tsuda K, Hamada S and Yoshimori T. Autophagy defends cells against invading group A Streptococcus. Science 306: 1037-40. 2004

32. Klionsky DJ, Abdelmohsen K and Abe A. Guidelines for the use and interpretation of assays for monitoring autophagy (3rd edition). Autophagy 12: 1-222. 2016
33. Young AR, Narita M, Ferreira M, Kirschner K, Sadaie M, Darot JF, Tavare S, Arakawa S, Shimizu S, Watt FM and Narita M. Autophagy mediates the mitotic senescence transition. Gene Dev 23: 798-803. 2009
34. Scherz-Shouval R and Elazar Z. ROS, mitochondria and the regulation of autophagy. Trends Cell Biol 17: 422-7. 2007
35. Chen QM. Replicative senescence and oxidant-induced premature senescence. Beyond the control of cell cycle checkpoints. Ann N Y Acad Sci 908: 111-25. 2000
36. Deacon K, Mistry P, Chernoff J, Blank JL and Patel R. p38 Mitogen-activated protein kinase mediates cell death and p21-activated kinase mediates cell survival during chemotherapeutic drug-induced mitotic arrest. Mol Biol Cell 14: 2071-87. 2003
37. Liu D and Xu Y. p53, oxidative stress, and aging. Antioxid Redox Signal 15(6): 1669-78. 2011
38. Lafarga V, Cuadrado A, Lopez de Silanes I, Bengoechea R, Fernandez-Capetillo O and Nebreda AR. p38 Mitogen-activated protein kinase- and HuR-dependent

stabilization of p21(Cip1) mRNA mediates the G(1)/S checkpoint. Mol Cell Biol 29: 4341-51. 2009

39. Stepniak E, Ricci R, Eferl R, Sumara G, Sumara I, Rath M, Hui L and Wagner EF. c-Jun/AP-1 controls liver regeneration by repressing p53/p21 and p38 MAPK activity. Gene Dev 20: 2306-14. 2006

40. Zhou YY, Li Y and Zhou LF. MAPK/JNK signalling: a potential autophagy regulateon pathway. Biosci Rep 35: e00199. 2015

41. Sohn D, Graupner V, Neise D, Essmann F, Schulze-Osthoff K and Janicke RU. Pifithrin-alpha protects against DNA damage-induced apoptosis downstream of mitochondria independent of p53. Cell Death Differ 16: 869-78. 2009

42. Mallette FA, Goumard S, Gaumont-Leclerc MF, Moiseeva O and Ferbeyre G. Human fibroblasts require the Rb family of tumor suppressors, but not p53, for PML-induced senescence. Oncogene 23: 91-9. 2004

43. Sun P, Yoshizuka N, New L, Moser BA, Li Y, Liao R, Xie C, Chen J, Deng Q, Yamount M, Dong MQ, Frangou CG, Yates JR 3rd, Wright PE and Han J. PRAK is essential for ras-induced senescence and tumor suppression. Cell 128: 295-308. 2007

44. Nishikawa T, Tsuno NH, Okaji Y, Shuno Y, Sasaki K, Hongo K, Sunami E, Kitayama J, Takahashi K and Nagawa H. Inhibition of autophagy potentiates sulforaphane-induced apoptosiss in human colon cancer cells. Ann Surg Oncol

17: 592-602. 2010

45. de Bruin EC and Medema JP. Apoptosis and no-apoptotic deaths in cancer development and treatment response. Cancer Treat Rev 34: 737-49. 2008

46. Yosef R, Pilpel N, Torarsky-Amiel R, Biran A, Ovadya Y, Vadal E, Dassa L, Shahar E, Condiotte R, Ben-Porath I and Krizhanovsku V. Directed eliminateon of senescent cells by inhibition of BCL-W and BCL-XL. Nat Commun 7: 11190. 2016

47. Cayrol C, Knibiehler M and Ducommun B. p 21 binding to PCNA causes G1 and G2 cell cycle arrest in p53-deficient cells. Oncogene 16: 311-20. 1998

48. Chen A, Huang, X, Xug Z, Cao D, Huang K, Chen J, Pan Y and Gao Y. The role of p21 in apoptosis, proliferation, cell cycle arrest, and antioxidant activety in UVB-irradiated human HaCaT keratinocytes. Med Sci Monit 21: 86-95. 2015

49. Karimian A, Admadi Y and Yousefi B. Multiple functions of p21 in cell cycle, apoptosiss and transcriptional regulation after DNA damage. DNA Repair 42: 63-71. 2016

Figure Legends

Figure 1. **Effect of H_2O_2 treatment on HaCaT cells**

(A) Cell viability was determined by trypan blue dye exclusion at the indicated times following treatment with 300 μM H_2O_2. All values are presented as the means ± SDs from five independent studies. *Significantly different at $P < 0.05$ compared with 12-72

hours (ANOVA followed by Scheffe's test). There are no significantly difference in groups jointed to horizon bars. (B) Representative phase contrast images of morphological changes in HaCaT cells treated with or without 300 μM H_2O_2 for 24 h. Arrows show the cytoplasmic granules. Bar = 50 μm.

Figure 2. H_2O_2 induces senescence in HaCaT cells

(A) Representative senescence-associated β-galactosidase (SA-β-gal) staining of HaCaT cells treated with or without 300 μM H_20_2 for 24 h. Bar = 50 μm. (B) SA-β-gal-positive cells were quantified by counting more than 100 cells for each sample. All values are means ± SDs from three independent studies. The control cells exhibited no detectable SA-β-gal staining. * Significantly difference at $P < 0.05$ compared with untreated cells (Student's t-test).

Figure 3. **Effect of H_2O_2 treatment on proliferative activity in HaCaT cells**

(A) Representative immunofluorescent images Ki-67-positive cells treated with or without 300 μM H202 for 24 h. Bar = 50 μm. (B) Ki-67-positive cells were quantified by counting more than 100 cells for each sample. All values are means ± SDs from three independent studies. * Significantly difference at $P < 0.05$ compared with untreated cells (Student's t-test).

Figure 4. **p21 and Decl expression in H_2O_2-treated HaCaT cells**

Western blot analyses of p21 and Dec1 in HaCaT cells treated with 300 μM H_2O_2 for the indicated times. β-actin (ACTB) was used as a loading control. The band density

was quantified and normalized to that of ACTB on 0 hour.

Figure 5. **Induction of autophagy in HaCaT cells by H_2O_2 stimulation.**

Western blot analysis of microtubule-associated protein light chain 3 (LC3 II) expression in HaCaT cells treated with 300 μM H_2O_2 for the indicated time periods. β-actin (ACTB) was used as a loading control. The band density was quantified and normalized to that of ACTB on 0 hour.

Figure 6. **Accumulation of autophagosomes in H_2O_2-treated cells**

(A) Representative immunofluorescence images of the accumulation of autophagosomes in HaCaT cells. The cells were incubated in the absence or presence of 300 μM H_2O_2 for 24 h, fixed in 4% paraformaldehyde, and immunolabeled with anti-LC3 antibody (1:100 dilution) followed by Alexa Fluor 488-conjugated goat anti-rabbit IgG (1:250 dilution, green). Hoechst 33342 was used for nuclear staining (blue). Bar = 100 μm. Ctr, untreated (control) cells. H_2O_2, treated cells. (B) Graph displays the percentage of HaCaT cells with LC3-positive autophagosomes. All values are means ± SDs from five independent studies. * Significantly difference at $P < 0.05$ compared with untreated cells (Student's t-test).

Figure 7. **Pretreatment with 3-methyladenine (3-MA) attenuates H_2O_2-induced autophagy and senescence**.

HaCaT cells were treated with 5 mM 3-MA for 2 h. After pretreatment, the cells were exposed to 300 μM H_2O_2 for 24 h. Representative Western blotting images of

microtubule-associated protein light chain 3 (LC3 I and II), p21, and Decades (Dec1) are shown. β-actin (ACTB) blot is included as a loading control. The band density was quantified and normalized to that of ACTB on cells treated without both H_20_2 and 3-MA.

Figure 8. **LC3 expression in HaCaT cells pretreatment with or without 3-methyladenine (3-MA).**

Representative fluorescence images of punctate LC3 expression in HaCaT cells. Bar = 50 μm.

Figure 9. **Pretreatment with 3-methyladenine (3-MA) attenuates H_2O_2-induced autophagic and senescent factors**

(A) Graph displays the percentage of HaCaT cells with punctate LC3 expression. All values are means ± SDs from five independent studies. Parallel bar indicates no significant difference. *Significantly different at $P < 0.05$ compared with untreated and 3-MA- treated cells (ANOVA followed by Scheffe's test). (B) The graphs display quantification of the percentages of senescence-associated β-galactosidase (SA-β-gal) – and Ki-67– positive cells. The data are presented as means ± SDs from five independent experiments. Parallel bar indicates no significant difference. *Significantly different at $P < 0.05$ compared with untreated and 3-MA-treated cells (ANOVA followed by Scheffe's test).

Figure 10. **No effect of H_2O_2 treatment on mammalian target of rapamycin (mTOR) pathways to increase autophagy.**

HaCaT cells were either treated with vehicle (Dulbecco's modified Eagle's medium with 10% fetal bovine serum) as a control (Ctr) or with 300 μM H_2O_2 for 24 h. Representative images of Western blotting analysis are shown. Levels of selective autophagic proteins (LC3 and Beclin-1, BECN1), the mTOR complex 1-phosphorylated products p-p70S6K and p-4E-BP1, and the mTOR complex 2- phosphorylated product p-AKT (s473) were analyzed by Western blots. β-actin (ACTB) was used as a loading control. The band density was quantified and normalized to that of ACTB on untreated cells (control).

Figure 11. **Intracellular reactive oxygen species (ROS) production in H_2O_2-treated HaCaT cells.**

HaCaT cells were either treated with 300 μM H_2O_2 alone or 300 μM H_2O_2 plus 100 mM N-acetylcystein (NAC) for 24 h. The cells treated with medium alone were control (Ctr). Representative immunofluorescence images are shown to demonstrate an intracellular ROS production (green). Nuclei were stained with Hoechst 33324 (blue). Bar = 50 μm.

Figure 12. **Intracellular reactive oxygen species (ROS) production regulates the induction of autophagy.**

Levels of autophagy-related factors, LC3-I and II and Beclin-1 (BECN1) analyzed by Western blotting. β-actin (ACTB) was used as a loading control. The band density was quantified and normalized to that of ACTB on untreated cells (control).

Figure 13. **Intracellular reactive oxygen species (ROS) production regulates the induction of cellular senescence.**

Levels of the senescence-related factors, p21 and Dec1were analyzed by Western blotting. β-actin (ACTB) was used as a loading control. The band density was quantified and normalized to that of ACTB on untreated cells (control).

Figure 14. **Acceleration of p38 mitogen-activated protein kinase α (MAPKα) activity in H_2O_2-treated HaCaT cells.**

HaCaT cells were either treated with 300 μM H_2O_2 alone or 300 μM H_2O_2 plus 100mM NAC. Immunoblotting assay was performed with antibodies against p53, phosphorylated -p53 (p-p53), p38 MAPKα, and phosphorylated-p38 MAPKα. β-actin (ACTB) was used as a loading control. The band density was quantified and normalized to that of ACTB on untreated cells (control).

Figure 15. **Effect of PFTa on p-p53 and p21 expression in H_2O_2-treated HaCaT cells.**

Levels of p-p53 and p21 expression analyzed by Western blotting. β-actin (ACTB) was used as a loading control. The band density was quantified and normalized to that of ACTB on untreated cells (control).

Figure 16. **Effect of SB203580 treatment on the expression of p-p38 MAPKα, p21, and LC3 in H_2O_2-treated cells.**

Western blotting analysis. The β-actin (ACTB) was used as a loading control. The band density was quantified and normalized to that of ACTB on untreated cells (control).

Figure 17. **Effect of SB203580 treatment on** SA-β-gal positive and Ki-67 positive cells

Graphs display the effect of SB203580 treatment on the percentage of SA- β -gal positive (left) and Ki-67 positive (right) cells. The data are presented as means ± SDs from three independent experiments. Parallel bar indicates no significant difference. *Significantly different at $P < 0.05$ compared with untreated and SB203580-treated cells (ANOVA followed by Scheffe's test).

Figure 18 **A suppression of autophagy induces apoptosis in H_2O_2-treated cells**

HaCaT cells were treated with or without 5 mM 3-MA for 2 h. After pretreatment, the cells were exposed to 300 μM H_2O_2 for 24 h. Dual flurorescent images of cleaved PARP (green) and annexin V (red) in the cells untreated (control) or treated with H_2O_2. The nucleus was stained with Hoechst 33324 (blue). Bars = 100 μm. Ctr, control (untreated); 3-MA, 3-Methyladenine.

Figure 19 **Autophagy suppression induces apoptotic markers in H_2O_2-treated cells.**

HaCaT cells were treated with or without 5 mM 3-MA for 2 h. PARP, cleaved PARP, Bcl-2, and Bax were analyzed by Western blotting. The β-actin (ACTB) was used as a

loading control. The band density was quantified and normalized to that of ACTB on untreated cells (control). Ctr, control (untreated); 3-MA, 3-Methyladenine.

Fig1.

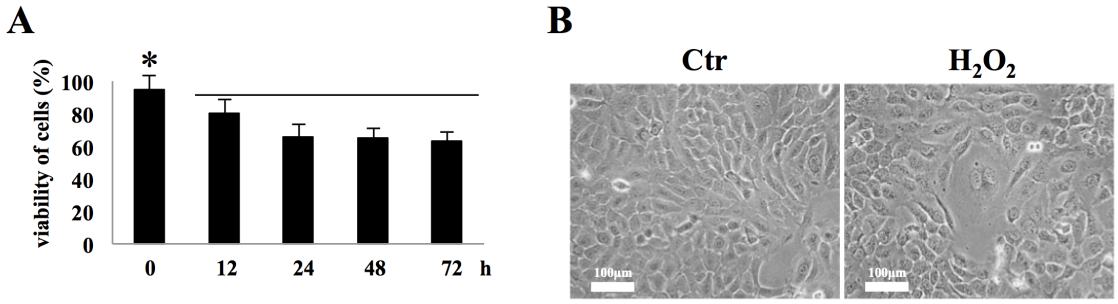

Fig2.

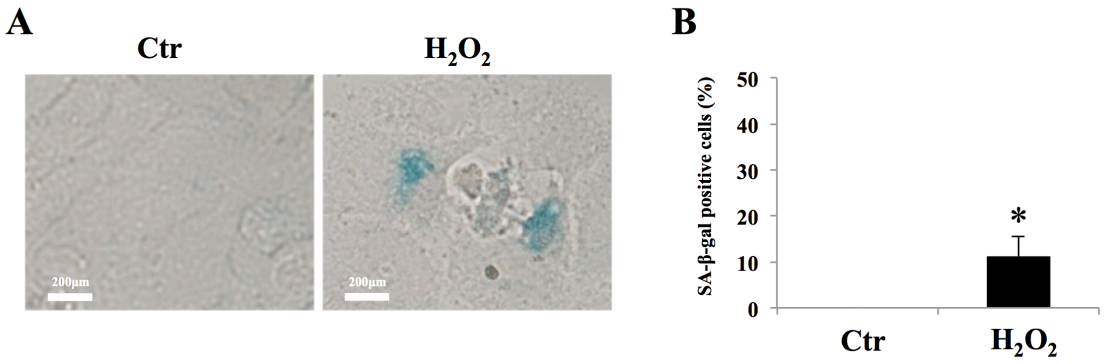

Fig3.

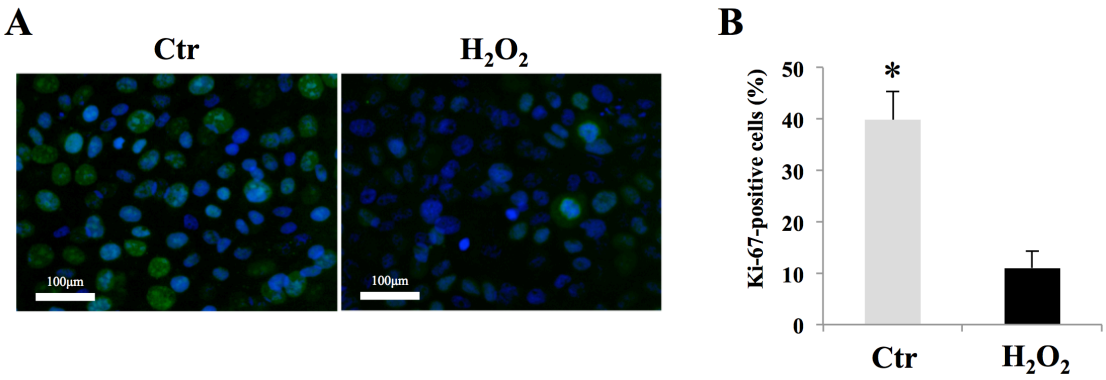

Fig4.

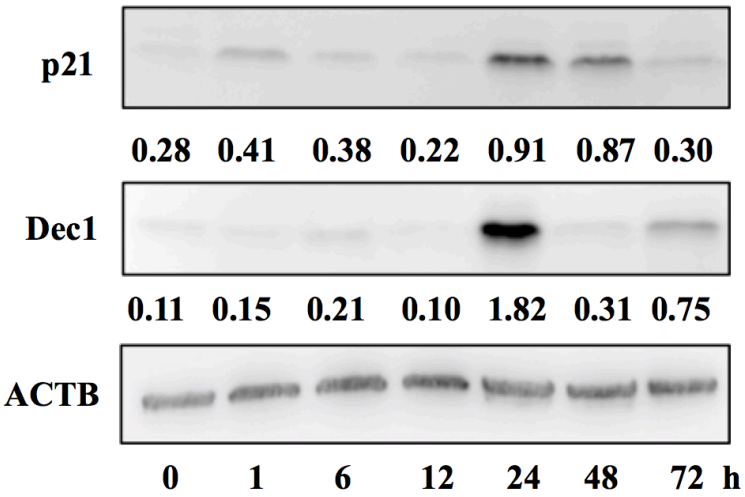
p21
0.28 0.41 0.38 0.22 0.91 0.87 0.30
Dec1
0.11 0.15 0.21 0.10 1.82 0.31 0.75
ACTB
0 1 6 12 24 48 72 h

Fig5.

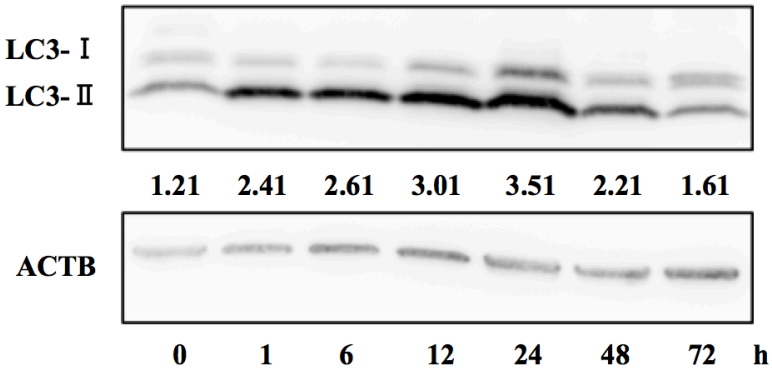
LC3- Ⅰ
LC3- Ⅱ
1.21 2.41 2.61 3.01 3.51 2.21 1.61
ACTB
0 1 6 12 24 48 72 h

Fig6.

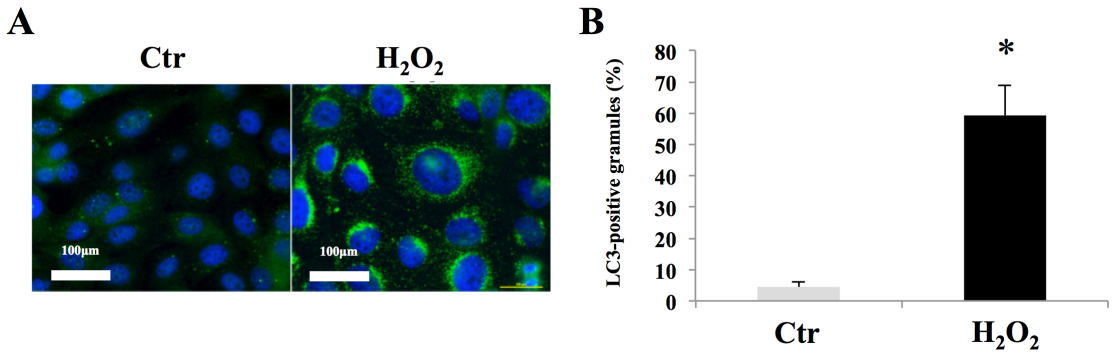
A
Ctr
H2O2
100μm
100μm
B
LC3-positive gramules (%)
80
70
60
50
40
30
20
10
0
*
Ctr
H2O2

Fig7.

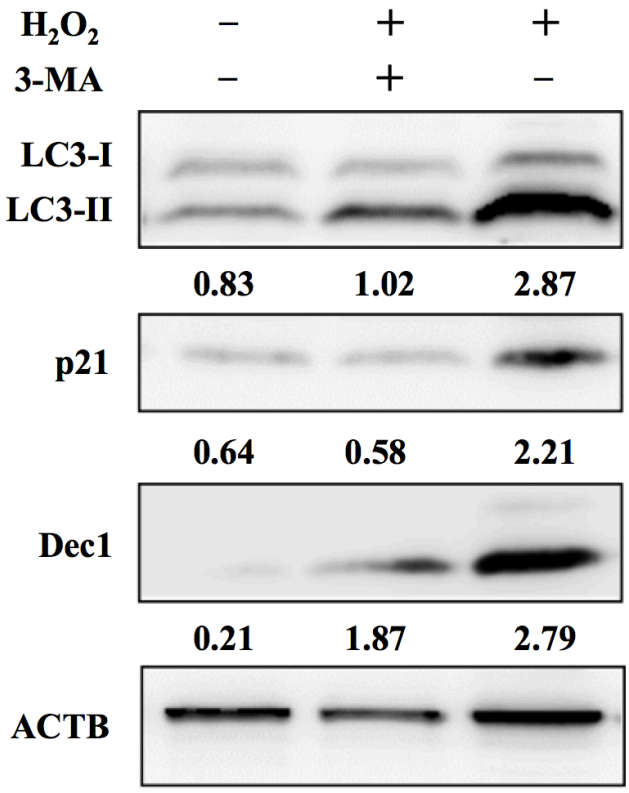
H2O2 − + +
3-MA − + −
LC3-I
LC3-II
0.83 1.02 2.87
p21
0.64 0.58 2.21
Dec1
0.21 1.87 2.79
ACTB

Fig8.

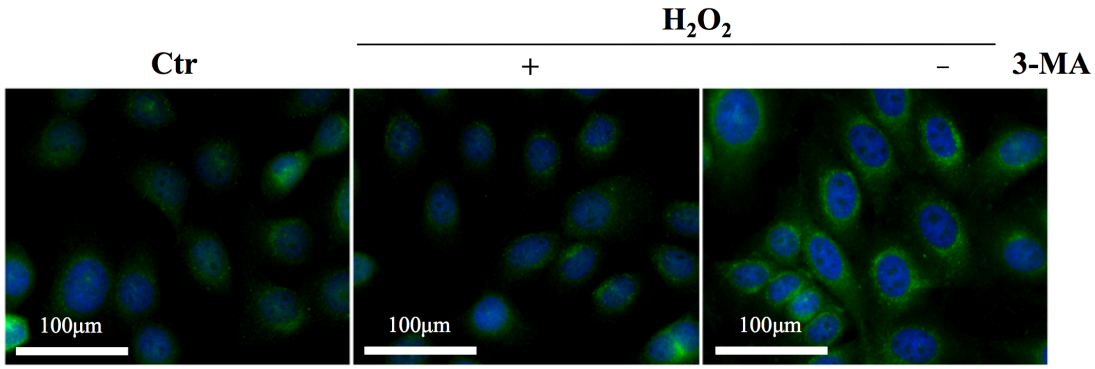
H2O2
Ctr
+
–
3-MA
100μm
100μm
100μm

Fig9.

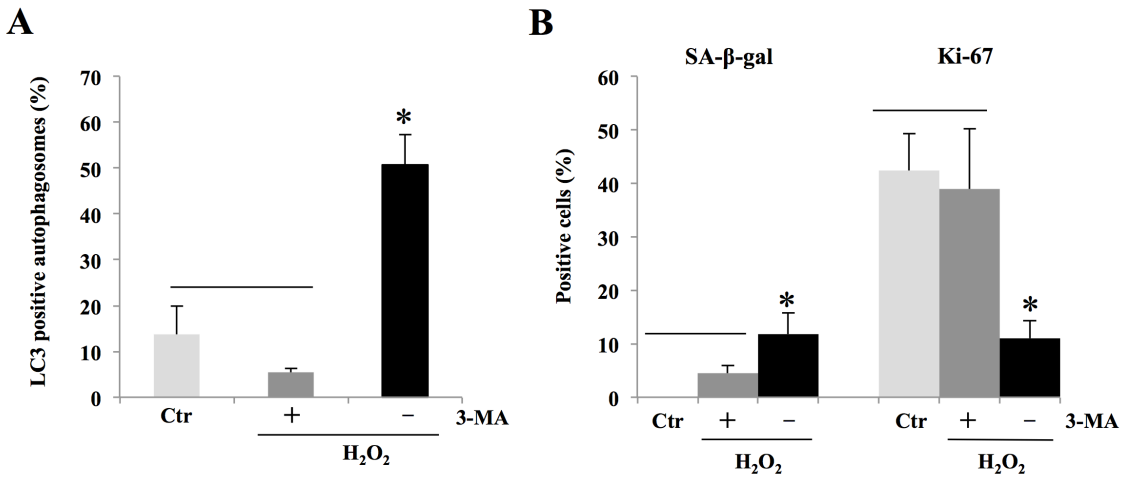
A
LC3 positive autophagosomes (%)
70
60
50
40
30
20
10
0
*
Ctr
+
–
3-MA
H2O2
B
SA-β-gal
Ki-67
Positive cells (%)
60
50
40
30
20
10
0
*
*
Ctr
+
–
Ctr
+
–
3-MA
H2O2
H2O2

Fig10.

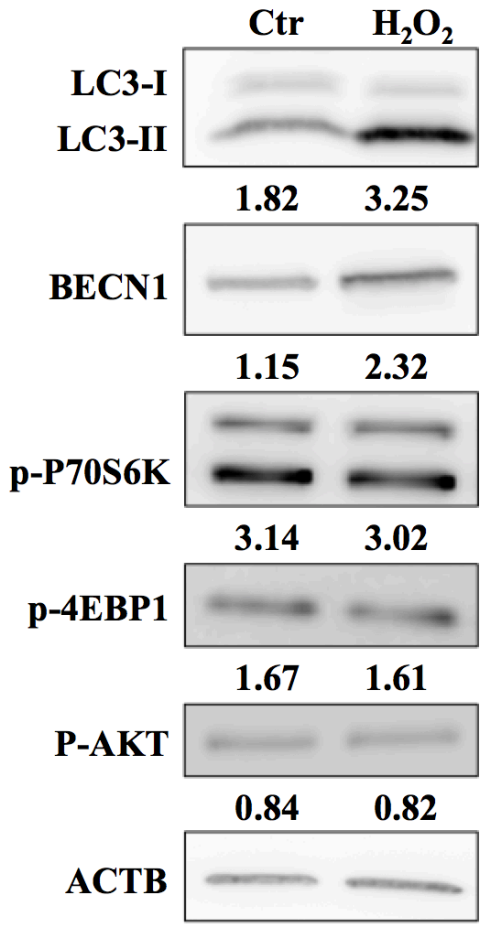
Ctr
H_2O_2
LC3-I
LC3-II
1.82
3.25
BECN1
1.15
2.32
p-P70S6K
3.14
3.02
p-4EBP1
1.67
1.61
P-AKT
0.84
0.82
ACTB

Fig11.

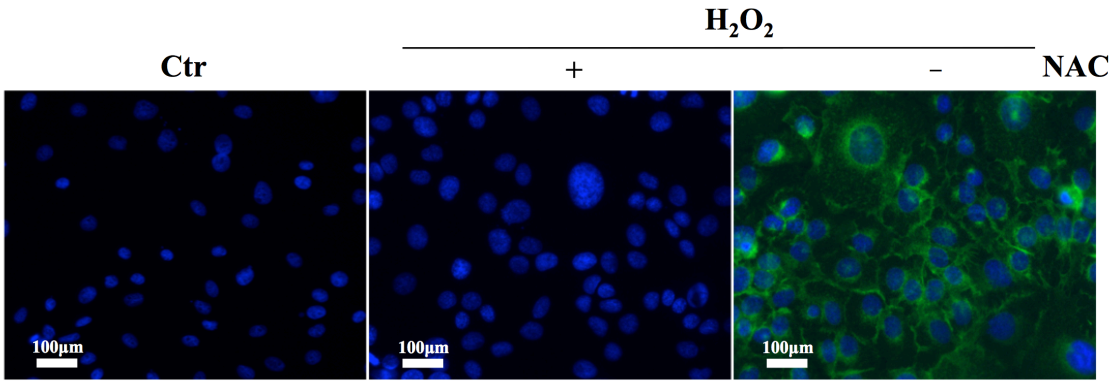
H_2O_2
Ctr
+
–
NAC
100μm
100μm
100μm

Fig12.

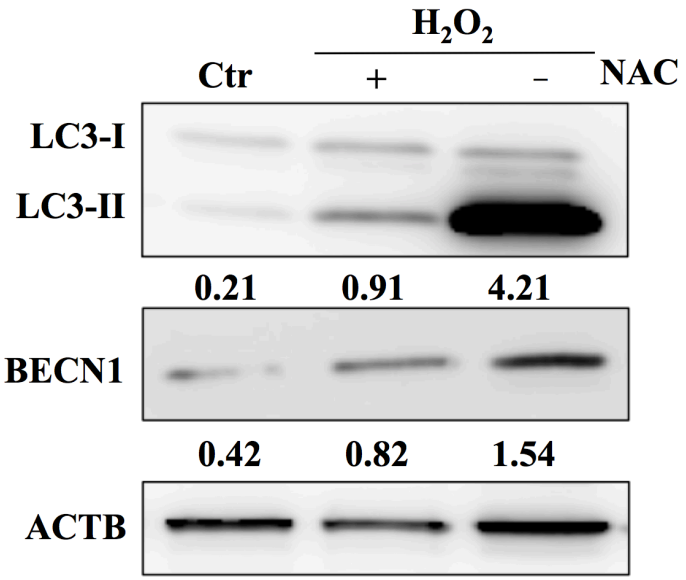
H2O2
Ctr
+
–
NAC
LC3-I
LC3-II
0.21
0.91
4.21
BECN1
0.42
0.82
1.54
ACTB

Fig13.

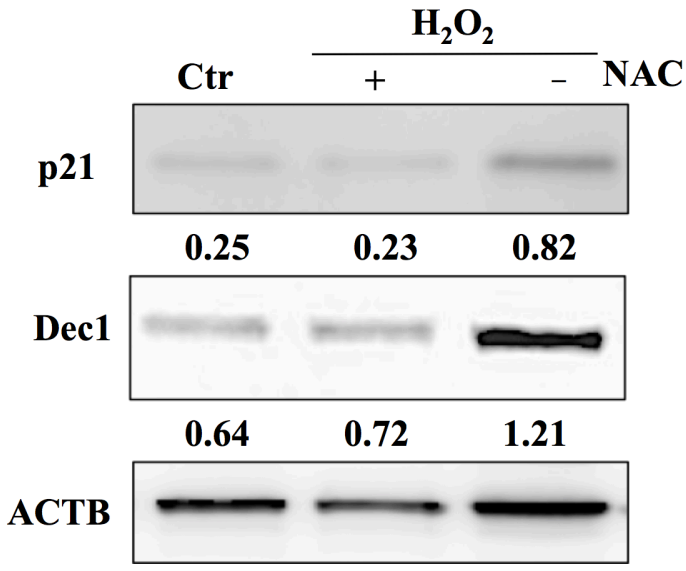
H2O2
Ctr
+
–
NAC
p21
0.25
0.23
0.82
Dec1
0.64
0.72
1.21
ACTB

Fig14.

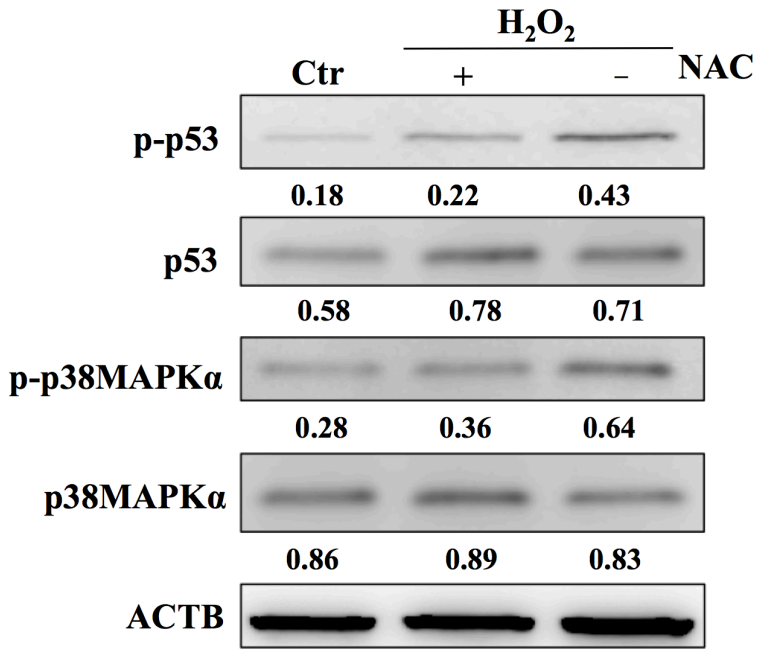
H2O2
Ctr
+
–
NAC
p-p53
0.18
0.22
0.43
p53
0.58
0.78
0.71
p-p38MAPKα
0.28
0.36
0.64
p38MAPKα
0.86
0.89
0.83
ACTB

Fig15.

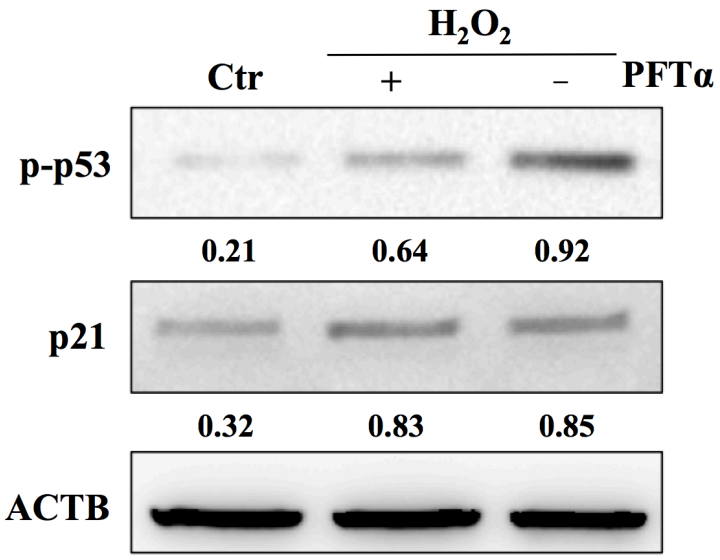
H2O2
Ctr
+
–
PFTα
p-p53
0.21
0.64
0.92
p21
0.32
0.83
0.85
ACTB

Fig16.

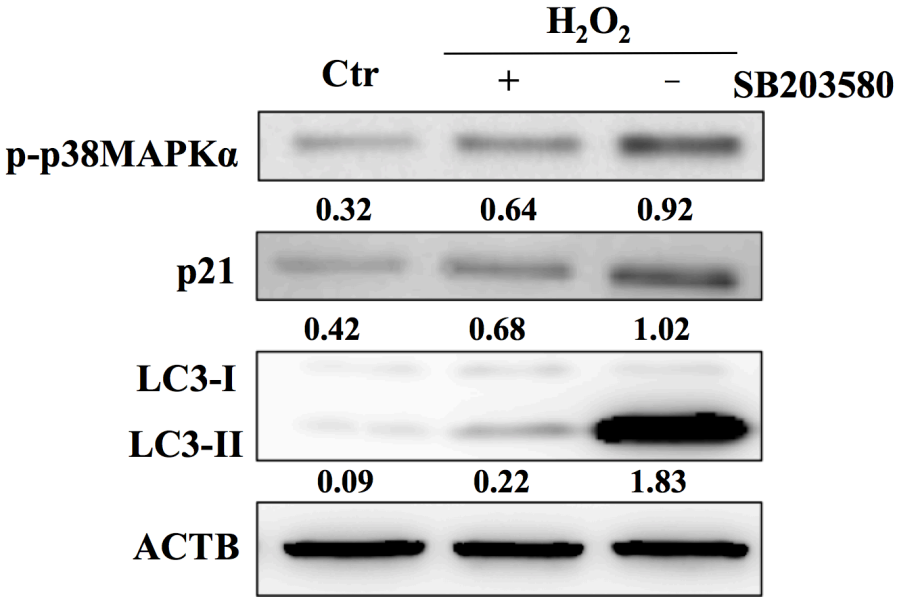
H2O2
Ctr
+
−
SB203580
p-p38MAPKα
0.32
0.64
0.92
p21
0.42
0.68
1.02
LC3-I
LC3-II
0.09
0.22
1.83
ACTB

Fig17.

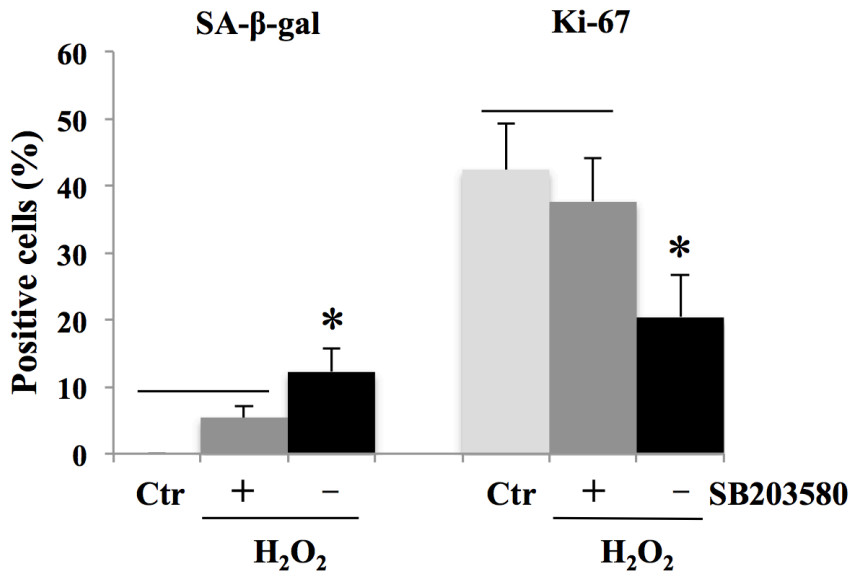
SA-β-gal
Ki-67
Positive cells (%)
60
50
40
30
20
10
0
*
*
Ctr
+
−
Ctr
+
−
SB203580
H2O2
H2O2

Fig18.

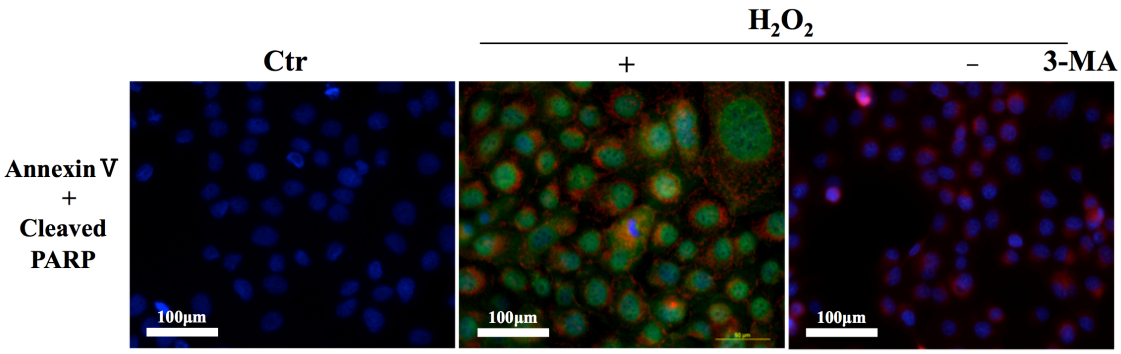
H_2O_2
Ctr
+
–
3-MA
Annexin V
+
Cleaved
PARP
100μm
100μm
100μm

Fig19.

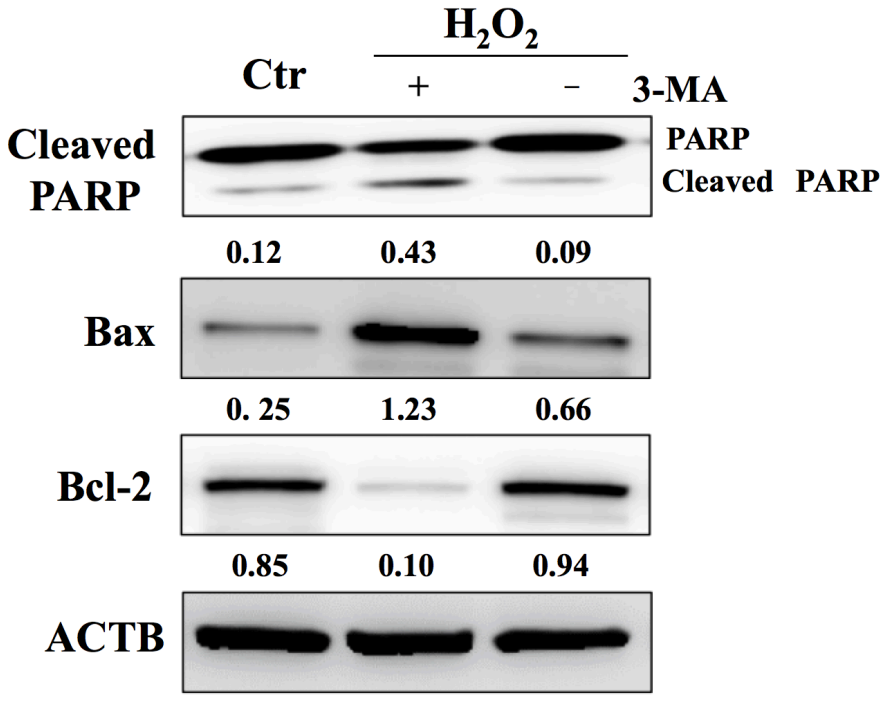
H_2O_2
Ctr
+
–
3-MA
Cleaved
PARP
PARP
Cleaved PARP
0.12
0.43
0.09
Bax
0. 25
1.23
0.66
Bcl-2
0.85
0.10
0.94
ACTB